

SparseTrack: Multi-Object Tracking by Performing Scene Decomposition based on Pseudo-Depth

Zelin Liu, Xinggang Wang, Cheng Wang, Wenyu Liu, Xiang Bai

Abstract— Exploring robust and efficient association methods has always been an important issue in multiple-object tracking (MOT). Although existing tracking methods have achieved impressive performance, congestion and frequent occlusions still pose challenging problems in multi-object tracking. We reveal that performing sparse decomposition on dense scenes is a crucial step to enhance the performance of associating occluded targets. To this end, we propose a pseudo-depth estimation method for obtaining the relative depth of targets from 2D images. Secondly, we design a depth cascading matching (DCM) algorithm, which can use the obtained depth information to convert a dense target set into multiple sparse target subsets and perform data association on these sparse target subsets in order from near to far. By integrating the pseudo-depth method and the DCM strategy into the data association process, we propose a new tracker, called SparseTrack. SparseTrack provides a new perspective for solving the challenging crowded scene MOT problem. Only using IoU matching, SparseTrack achieves comparable performance with the state-of-the-art (SOTA) methods on the MOT17 and MOT20 benchmarks. Code and models are publicly available at <https://github.com/hustvl/SparseTrack>.

Index Terms— 2D multi-object tracking, occluded object tracking, scene decomposition, and data association.

I. INTRODUCTION

MULTI-object tracking (MOT) [1] has vast applications in fields such as autonomous driving, surveillance, and intelligent transportation. It aims to consistently identify the same object in different video frames as the same identity in the form of bounding boxes. Although previous trackers have achieved high performance on multiple tracking datasets [2]–[4], dense crowds and frequent occlusions still make multi-object tracking tasks challenging.

Current mainstream tracking methods follow the paradigm of tracking-by-detection (TBD) [5] and perform frame-by-frame data association. In order to solve the obstacle of occlusion association in dense scenes, some simple methods, such as ByteTrack [6], have achieved effective tracking of occluded targets in dense scenes by separately associating low-score detections. Although ByteTrack demonstrates proficiency in processing low-score detections separately, its accuracy in location association is prone to deterioration in scenes characterized by a high volume of low-score occlusions or frequent overcrowding, as shown in Fig. 1. Other methods [7]–[12] ensure tracking performance of occluded instances by using

Z. Liu, X. Wang, C. Wang, W. Liu and X. Bai are with Huazhong University of Science and Technology, China.

Corresponding author: Xinggang Wang. Email: xgwang@hust.edu.cn.



Fig. 1. An illustration of associating low-score detections in crowded scenes. In ByteTrack [6], a set of low-score detections are matched with the track set at the same time using the IoU metric, which is easy to make mistakes due to the high location similarity between the low-score detections. This paper attempts to solve this problem from the low-score detection decomposition perspective rather than matching them at the same time.

powerful temporal modeling and trajectory query mechanisms. However, these methods are typically associated with high computational costs, particularly in scenes populated by a multitude of objects and frequent occlusions.

In this work, we prove that the target set decomposition based on depth information is an effective approach for dealing with dense occlusions in data association. As illustrated in Fig. 2, we show an occlusion order for the objects in a local region and the occlusion order is consistent with the depth order, from near to far. Thus, a set of dense occlusions can be divided into several non-overlapping subsets by utilizing a segmentation strategy based on depth information. Between adjacent target subsets, their x - y locations could be similar, but their x - y -depth locations can be much easier to distinguish. The tracker performs data association separately for sparse subsets at different depth levels. Compared to directly associating the entire occluded object set at the same time, the sparse decomposition would be more effective for alleviating the collision probability of trajectories with similar positions but different depths during data association. Specifically, we prioritize the association of target subsets with smaller depths since the occlusion order is highly correlated with the depth order. As a result, the targets in each subset can be handled in a fine-grained manner and be less affected by the targets in other depth levels.

To realize the above designs, we propose a method for obtaining the relative depth of targets from 2D images: the pseudo-depth method, which is based on two scene priors: 1) the camera that captures objects is higher than the ground, 2) all objects in the scene are on flat ground. In other words,

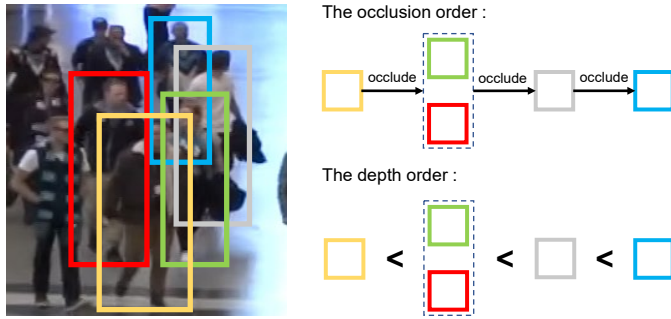


Fig. 2. An illustration of the occlusions at the local regions. As the depth value increases, the ranking of occluded targets gradually shifts toward the background.

there are no obvious undulations on the ground. In this case, we can project the relative depth of targets from 3D space onto the 2D image plane and obtain target pseudo-depth values, which is the distance from the bottom of the target bounding box to the bottom edge of the image. Notably, the pseudo-depth value is used as a reference to measure the relative depth relationship between targets using the ground as a reference system, rather than the ground truth depth of the target in 3D space. Furthermore, we design a depth cascade matching (DCM) algorithm to execute hierarchical association based on the target pseudo-depth information. Specifically, we divide trajectories and detections into multiple target subsets according to the distribution of pseudo-depth value. The DCM algorithm performs IoU [13] association on these sparse target subsets in the order of pseudo-depth value from nearest to farthest. By integrating the pseudo-depth method and DCM into the data association process, we propose a novel tracker called SparseTrack. The essence of SparseTrack lies in associating occlusions hierarchically based on depth via the DCM, as shown in Fig. 3.

SparseTrack achieves impressive performance on multiple tracking datasets, which proves the effectiveness of target set decomposition based on pseudo-depth. We take ByteTrack as a baseline. On the MOT17 [3] test set, SparseTrack achieved 65.1 HOTA [14], 81.0 MOTA, and 80.1 IDF1, which are gains of **+2.0** HOTA, **+0.7** MOTA, and **+2.8** IDF1 compared to the baseline. On the MOT20 [4] dataset, SparseTrack achieved 63.4 HOTA, 78.2 MOTA, and 77.3 IDF1, which are gains of **+2.1** HOTA, **+0.4** MOTA, and **+2.1** IDF1 compared to the baseline. Furthermore, we evaluate SparseTrack on DanceTrack [15] benchmark and obtain a gain of **+7.8** HOTA, **+1.7** MOTA, **+4.4** IDF1 compared to the baseline. It is worth noting that our proposed DCM algorithm is plug-and-play and can be integrated into different trackers, resulting in consistent performance improvements. The specific details are discussed in the experimental section.

Our contributions are summarized as follows:

- We propose a method for obtaining the relative depth of targets from 2D images: the pseudo-depth method, which is based on two prior in the scene, and can effectively obtain the pseudo-depth value of the target to compare the relative depth relationships between different objects.
- Based on the depth information provided by the pseudo-

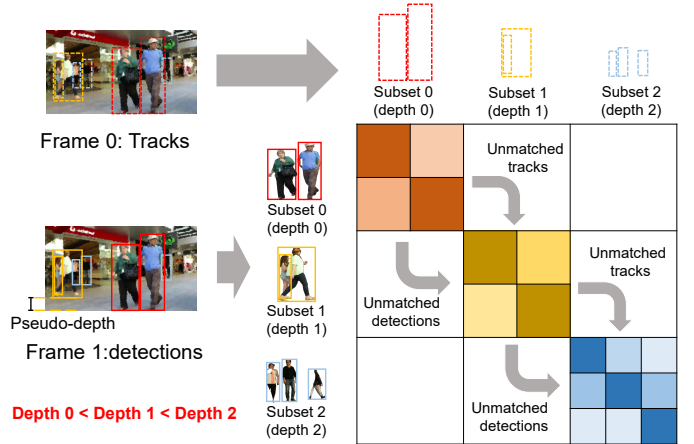


Fig. 3. An simple example of the hierarchical association from DCM, where the white square regions indicate that no data association is performed between the corresponding detection and trajectory subsets along both horizontal and vertical directions. The darkness of the square regions reflects the similarity between trajectories and detections, with darker colors indicating higher similarity. DCM decomposes the target set into multiple subsets according to depth order from near to far and performs data association on the detection and trajectory subsets at the same depth level. For the unmatched trajectories and detections from each depth level, the tracker will process them at the next depth level.

depth method, we design an effective depth cascade matching approach for associating occlusions in dense scenes. It can decompose dense target sets into multiple sparse target subsets to achieve scene decomposition.

- Based on the aforementioned design, we propose a new IoU-only tracker named as SparseTrack, which significantly outperforms the previous IoU-only trackers and achieves comparable results with recent state-of-the-art MOT methods on a wide range of MOT benchmarks.

II. RELATED WORK

A. 2D Multi-Object Tracking

Current research in 2D multi-object tracking is primarily focused on ensuring reliable data association, which can lead to the development of various tracking methods. These methods can be broadly classified into two categories based on the tracking clues: appearance features and motion information. Some trackers [16]–[19] use a powerful and robust Re-Identification (ReID) model [20]–[23] to alleviate the problems of occlusion and object disappearing. Although the ReID model incurs additional computational costs, the ReID model obtained by self-supervised pre-training [24]–[28] can effectively against the poor appearance of occluded targets and provide high-quality instance appearance embeddings for the tracker. Other trackers, such as [5], [11], [12], [29]–[35], either model the temporal information of objects using a Kalman filter [36] motion model based on the constant velocity assumption or use learnable temporal modules to learn motion clues of the object. These methods strive to provide robust appearance information and reliable temporal information to ensure tracking accuracy. SparseTrack follows the paradigm of tracking-by-detection and uses a simple Kalman filter as a motion model.

B. Methods for Handling Object Occlusion

The performance of a tracker is to some extent dependent on the ability to handle occlusions. Recent works have attempted to tackle occlusion from different perspectives. For example, MotionTrack [37] learns the motion pattern of trajectories and combines it with historical information to effectively handle occlusions. MOTR [11], an end-to-end MOT framework, processes new appearing targets and tracked targets separately using detection queries and trajectory queries, respectively, with a multi-frame training manner. Due to the relative independence between queries and sufficient temporal training, MOTR can perform well in temporal modeling of occlusions across time steps. BoT-SORT [34] combines camera motion compensation (CMC) and IoU-ReID fusion, which can integrate motion and appearance clues of the object for achieving accurate tracking of occlusions. SparseTrack provides a completely different solution for occlusion by performing the target set decomposition to ensure tracking performance of occlusions.

C. Targets Set Decomposition

Actually, many trackers that follow the tracking-by-detection paradigm perform some degree of the target set decomposition. For example, DeepSORT [29] achieves step-by-step association of the detection set through multi-stage cascaded matching. FairMOT [32] processes the detection set separately based on appearance and position clues, which can also be seen as a division of the detection set via tracking clues. ByteTrack [6] divides the detection set into high-score and low-score detections based on confidence scores, and uses the correlation between scores and occlusions to separately process low-score occluded targets. However, in dense crowds, congestion leads to occlusions, which results in low-score detections. Although ByteTrack decouples low-score occlusions from the scene, low-score targets are still crowded. In this case, IoU-based data association is prone to matching errors that limit the tracking ability to handle occlusions. To this end, SparseTrack divides the detection set and the trajectory set based on the pseudo-depth level to ensure that targets in each association step are no longer crowded.

D. The Applications of Depth Information in MOT

Depth information is commonly used in applications related to 3D scenes, such as monocular or stereo depth estimation, 3D detection and tracking, and recently popular neural radiance fields [38]. The standard depth provides abundant information on the appearance and position of objects, leading to different 3D tracking methods. For instance, TrackRCNN [39] uses appearance and motion features for tracking and enhances accuracy and stability by alternately tracking objects in 2D images and 3D point clouds. FANTrack [40] employs a feature-based association network (FAN) for object tracking, where features come from a 3D convolutional neural network (CNN) [41] for point cloud data and a 2D CNN for camera images. CenterPoint [42] uses a keypoint detector to detect the center of an object and regress to other attributes, including

3D size, 3D direction, and speed. Then, it performs 3D object tracking via simple greedy nearest point matching. In fact, a 2D image can be considered as the projection of a 3D scene under perspective transformation. According to the camera model, we can easily infer the variable relationship between a 2D image and a 3D scene. SparseTrack leverages this variable relationship to obtain the pseudo-depth values of targets in 2D image, which partially replace the role of standard depth in describing the position relationships among objects. To the best of our knowledge, SparseTrack is the first method that utilizes depth information to enhance 2D multi-object tracking.

III. METHOD

A. General Framework

SparseTrack follows the paradigm of tracking-by-detection and performs frame-by-frame data association. The overall framework is shown in Fig. 4. Given a frame f_i in a video sequence, it is first processed by the YOLOX [43] detector, which outputs detection results in the form of bounding boxes (x_1, y_1, x_2, y_2) and confidence scores s . Then based on each detected bounding box and input image size, we use the pseudo-depth method to obtain pseudo-depth values of targets in the 2D image. The specific details are described in Sec. III-B. Pseudo-depth values can reflect the relative depth relationship between targets in the image. In the data association process, we utilize the pseudo-depth values of the detection and trajectory instances and use the DCM algorithm described in Sec. III-C to accomplish the decomposition and association for the tracks and the detections, separately. Finally, SparseTrack outputs tracking results as (x_1, y_1, w, h, s) , where the coordinates (w, h) represent the width and height of instance bounding boxes.

B. Pseudo-Depth Method

The starting conditions of pseudo-depth method is based on two prior assumptions in general tracking scenes: the camera that captures objects is above the ground and all objects in the scene are on the same plane. These assumptions are easily satisfied in general scenarios. Specifically, pseudo-depth method is a simple geometric method for obtaining pseudo-depth values. Firstly, we acquire the position point P_0 where the object in 3D space contacts the ground, project point P_0 onto the image plane F of the camera, and obtain the corresponding projection point P_1 . Secondly, we draw a perpendicular from point P_1 to the bottom edge L_b of the image and obtain the intersection point D between the perpendicular and the bottom edge L_b . We define the Euclidean distance between the projection point P_1 and the intersection point D as the pseudo-depth value of objects, as shown in Fig. 5. The pixel coordinates of P_1 and D are denoted as (x_p, y_p) and (x_d, y_d) , respectively. The pseudo-depth is computed as:

$$L_p = \sqrt{(x_p - x_d)^2 + (y_p - y_d)^2}, \quad (1)$$

where L_p is the pseudo-depth value. Although pseudo-depth values can not represent the ground truth depth of the target in

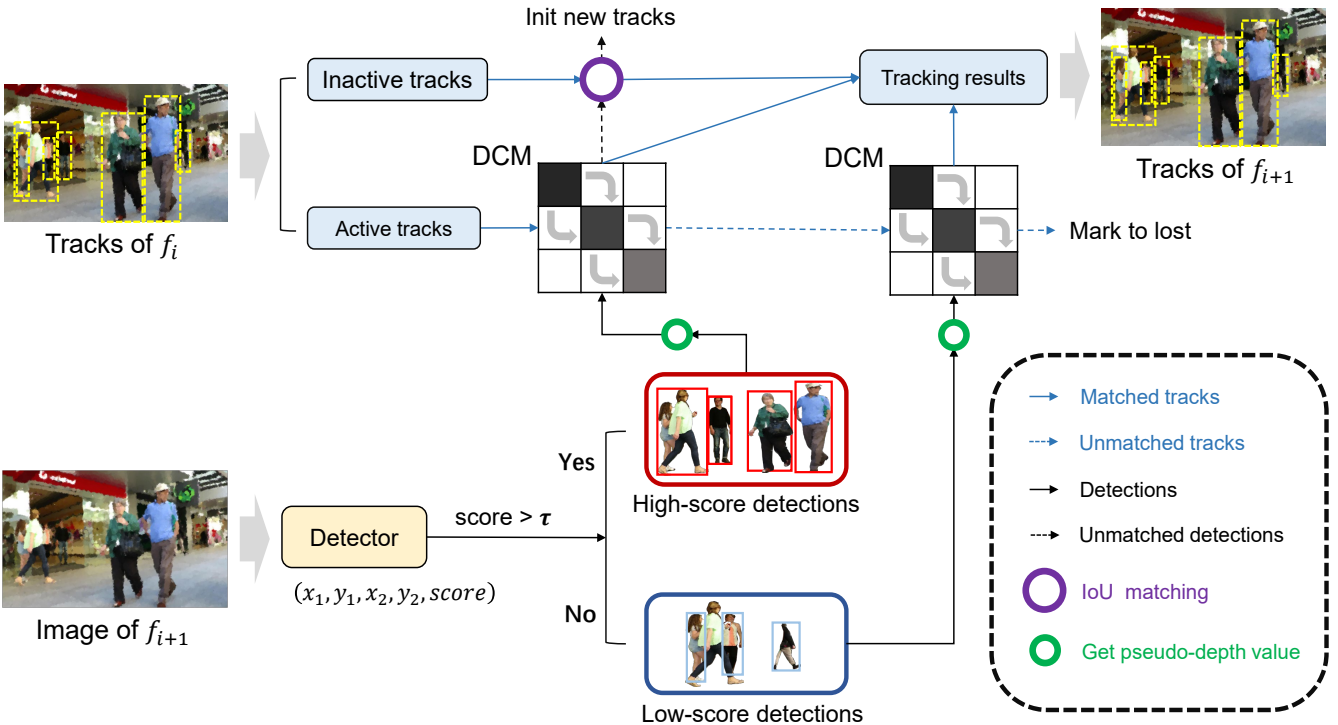


Fig. 4. The overall framework of SparseTrack. The legend information is located in the box at the bottom right corner. τ is used to divide high-score and low-score detections. SparseTrack performs the target set decomposition to associate low-score occlusions accurately via DCM and pseudo-depth method.

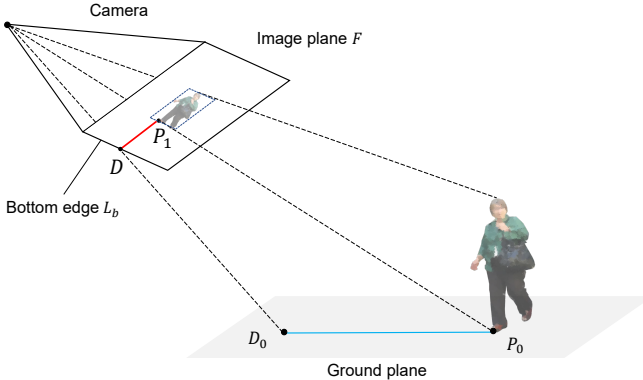


Fig. 5. The illustration of pseudo-depth method. The pseudo depth value is equal to the euclidean distance between P_1 and D . In fact, pseudo-depth can be regarded as a projection that can be obtained by projecting the distance between P_0 and D_0 in 3D space onto the image plane. In the projection transformation, since the euclidean distance between P_0 and D_0 is positively correlated with the pseudo-depth value, the pseudo-depth can reflect the depth of the target in the scene.

3D space, it is able to sufficiently measure the relative depth relationship between different objects on the same ground, which also provides a basis for dense crowd division at the depth level.

C. Depth Cascade Matching

With the depth information obtained by the pseudo-depth method, we can divide targets in the scene based on their pseudo-depth values, resulting in a sparser distribution of previously dense crowds. Firstly, we compute the minimum

pseudo-depth value of the detection set D_{d-min} and the maximum pseudo-depth value of the detection set D_{d-max} . Then we uniformly divide the interval distance between D_{d-min} and D_{d-max} into k depth intervals $\{I_0, I_1, \dots, I_{k-1}\}_{det}$, which serve as k different depth levels. With the same method, we can also obtain the minimum pseudo-depth value of the trajectory set D_{t-min} , maximum pseudo-depth value of the trajectory set D_{t-max} , and k depth intervals $\{I_0, I_1, \dots, I_{k-1}\}_{track}$. Based on the detection depth intervals $\{I_0, I_1, \dots, I_{k-1}\}_{det}$ and the track depth intervals $\{I_0, I_1, \dots, I_{k-1}\}_{track}$, we separately obtain the trajectory subsets T_{sub} and detection subsets D_{sub} that are located at different depth levels according to pseudo-depth values. Subsequently, the tracker performs IoU association \mathcal{I} between the trajectory and detection subsets at the same depth level. Unmatched trajectories T_0 and detections D_0 will participate in the association process of the next depth level after the data association at each depth level. The pseudo-code of the depth cascade matching algorithm is shown in Algorithm 1.

D. The Association Process of SparseTrack

We propose a simple yet powerful data association method. Unlike other methods [17], [29], [32], [33], [44]–[46] that focus on improving the appearance features and motion cues to ensure the reliability of association, SparseTrack divides all targets in the scene into multiple sparse target subsets by the pseudo-depth method and DCM to effectively associate occlusions in crowds. We first divide the detection set into high-score and low-score detection subsets based on confidence scores. Then, we use the aforementioned depth cascaded matching algorithm to perform data association on

Algorithm 1: Depth Cascade Matching.

Input: tracks set T ; detections set D ; the number of depth levels k ; Hungarian matching \mathcal{H} ; the function of IoU distance metric \mathcal{I} ; the function of getting max pseudo-depth value \mathcal{M}_{max} ; the function of getting min pseudo-depth value \mathcal{M}_{min} ; initialize matching threshold τ

Output: Matched tracks \mathcal{T} ; Unmatched tracks \mathcal{T}_0 ; Unmatched detections \mathcal{D}_0

```

1 Initialization:  $\mathcal{T} \leftarrow \emptyset, \mathcal{T}_0 \leftarrow \emptyset, \mathcal{D}_0 \leftarrow \emptyset$ 
2 /* generate sparse subsets of detections */
3  $D_{d-max} \leftarrow \mathcal{M}_{max}(D)$ 
4  $D_{d-min} \leftarrow \mathcal{M}_{min}(D)$ 
5  $\{I_0, \dots, I_{k-1}\}_{det} \leftarrow split([D_{d-min}, D_{d-max}], k)$ 
6 for  $\{I_i\}_{det}$  in  $\{I_0, \dots, I_{k-1}\}_{det}$  do
7    $D_i \leftarrow \emptyset$ 
8   for  $d$  in  $D$  do
9     if  $d.depth \in \{I_i\}_{det}$  then
10       $D_i \leftarrow D_i \cup d$ 
11    end
12  end
13   $D_{sub} \leftarrow D_{sub} \cup D_i$ 
14 end
15 /* generate sparse subsets of tracks */
16  $D_{t-max} \leftarrow \mathcal{M}_{max}(T)$ 
17  $D_{t-min} \leftarrow \mathcal{M}_{min}(T)$ 
18  $\{I_0, \dots, I_{k-1}\}_{track} \leftarrow split([D_{t-min}, D_{t-max}], k)$ 
19 for  $\{I_i\}_{track}$  in  $\{I_0, \dots, I_{k-1}\}_{track}$  do
20    $T_i \leftarrow \emptyset$ 
21   for  $t$  in  $T$  do
22     if  $t.depth \in \{I_i\}_{track}$  then
23        $T_i \leftarrow T_i \cup t$ 
24     end
25   end
26    $T_{sub} \leftarrow T_{sub} \cup T_i$ 
27 end
28 /* depth cascade matching */
29 for track subset  $T_i$ , detection subset  $D_i$  in  $(T_{sub}, D_{sub})$  do
30   /* unmatched objects from previous stage
31   participate the association of current
32   stage. */
33    $T_i \leftarrow T_i \cup \mathcal{T}_0$ 
34    $D_i \leftarrow D_i \cup \mathcal{D}_0$ 
35   /* get cost matrix based on IoU distance */
36    $C_i \leftarrow \mathcal{I}(T_i, D_i)$ 
37   /* association */
38    $T_{matched}, \mathcal{T}_0, \mathcal{D}_0 \leftarrow \mathcal{H}(C_i, \tau)$ 
39   /* add matched tracks */
40    $\mathcal{T} \leftarrow \mathcal{T} \cup T_{matched}$ 
41 end
42 Return:  $\mathcal{T}, \mathcal{T}_0, \mathcal{D}_0$ 

```

the high-score detection subset. For trajectories that appear in the previous frame but are not matched, we associate them with the low-score detection subset via the depth cascade matching algorithm. For unmatched high-score detections, we associate it with newly appeared trajectories in the previous frame. Finally, unmatched high-score detections are initialized as new trajectories, while lost trajectories that exceed the max

Algorithm 2: The Data Association of SparseTrack.

Input: A video sequence V ; object detector Det ; high-score detection threshold τ ; the function of depth cascade matching DCM ; the Kalman motion model KF

Output: tracking results of the video \mathcal{T}

```

1 Initialization:  $\mathcal{T} \leftarrow \emptyset$ 
2 for frame  $f_i$  in  $V$  do
3   /* get high-score and low-score detections
3    from current frame */
4    $D_i \leftarrow \text{Det}(f_i)$  /* detections per frame */
5    $D_{high} \leftarrow \emptyset$ 
6    $D_{low} \leftarrow \emptyset$ 
7   for  $d$  in  $D_i$  do
8     if  $d.score > \tau$  then
9        $D_{high} \leftarrow D_{high} \cup \{d\}$ 
10    end
11  else
12     $D_{low} \leftarrow D_{low} \cup \{d\}$ 
13  end
14 end
15 /* predict the location of tracks from
16 previous frames */
16  $\mathcal{T} \leftarrow \text{KF}(\mathcal{T})$ 
17 /* associate high-score detections by DCM */
18  $T_{matched}, D_{unmatched} \leftarrow \text{DCM}(\mathcal{T}, D_{high})$ 
19  $T_{unmatched} \leftarrow \emptyset$ 
20 for  $t$  in  $(\mathcal{T} - T_{matched})$  do
21   if  $t.state$  is not lost then
22      $T_{unmatched} \leftarrow T_{unmatched} \cup \{t\}$ 
23 end
24 /* associate low-score detections by DCM */
25  $T_{re-matched} \leftarrow \text{DCM}(T_{unmatched}, D_{low})$ 
26 /* update tracking results */
27  $\mathcal{T} \leftarrow \{T_{matched}, T_{re-matched}\}$ 
28 /* add new tracks */
29 for  $d$  in  $D_{unmatched}$  do
30    $\mathcal{T} \leftarrow \mathcal{T} \cup \{d\}$ 
31 end
32 end
33 Return:  $\mathcal{T}$ 

```

Track confirmation is not shown in the pseudo-code for simplicity. Function DCM can refer to Algorithm 1. The key steps of SparseTrack are in green.

number of losing frames are removed. The pseudo-code of data association of SparseTrack is shown in Algorithm 2.

As the confidence score is related to the occlusion of the target, we inherit the decomposition method based on the confidence score from [6]. Since high-score detections often mean a lower degree of occlusion, we set the number of pseudo-depth levels to 1 or 2 during associating high-score objects. Conversely, for associating low-score detections, we set the number of pseudo-depth levels to 4 or 8, which helps in the fine-grained association of dense occlusions. It is worth mentioning that the DCM is plug-and-play and can be integrated into various trackers. The specific settings are detailed in Sec. IV.

IV. EXPERIMENTS

A. Setting

1) *Datasets*: We evaluate SparseTrack on the MOT17 [3], MOT20 [4], and DanceTrack [15] benchmark datasets, and submit the evaluation results to compare the performance with other methods. For ablation experiments, we split half of the training sets of MOT17 and MOT20 (dense scene) as validation sets to evaluate the performance of different components. We also integrate DCM into seven different trackers and validate the effectiveness of our proposed method on the validation set of MOT17.

2) *Metrics*: We use the common CLEAR metrics [47] (MOTA, FP, FN, IDs, *etc.*), IDF1 [48], HOTA [14], AssA and DetA, to evaluate tracking performance. MOTA is computed based on FP, FN, and IDs. As the number of FP and FN is larger than that of IDs, MOTA prefers to reflect detection performance. Additionally, IDF1 and AssA focus more on association performance. DetA is used to measure detection accuracy. HOTA is a comprehensive measure used to evaluate the overall effectiveness of detection and association.

3) *Implementation details*: During the data association stage, we set different numbers of pseudo-depth levels for different datasets according to the scene crowding level. For MOT17, we set the default number of pseudo-depth levels to 3 and keep the maximum length of lost tracks at 30 frames. For MOT20, we set the default number of depth levels to 8 and keep the maximum length of lost tracks at 60 frames. For DanceTrack, we set the number of depth levels to 12 and keep the lost tracks until 60 frames. The high-score detection threshold is set to 0.6 by default. To align the positions of detections and tracks on depth levels as closely as possible, we implement a fast online version of global motion compensation (GMC) based on BoT-SORT [34]. It is worth noting that all our experimental results rely on IoU distance association and do not use any appearance feature component.

To make a fair comparison with the baseline method [6] in the detection stage, we adopt the YOLOX [43] detector and use the same weights and training configuration as the baseline method. For evaluating on the MOT17 test set, we train SparseTrack on the combination of ETHZ [49], CrowdHuman [50], CityPersons [51] and MOT17 train set. For evaluating on the MOT20 test set, we train SparseTrack on the combination of CrowdHuman and MOT20 train set. For evaluating on the MOT17 validation set, we train SparseTrack on the combination of CrowdHuman and the half of MOT17 train set. For the evaluation on the MOT20 validation set, we train SparseTrack on the CrowdHuman and the half of MOT20 train set. Furthermore, we train SparseTrack on the combination of train set and val set from DanceTrack, and evaluate the performance on test set of DanceTrack. All implementations are performed on NVIDIA GeForce RTX 3090 GPUs.

B. Evaluation of Different Benchmark

We evaluate SparseTrack on the test set of MOT17, MOT20 and DanceTrack to compare with other methods. All evalua-

TABLE I
THE COMPARISON OF SPARSETRACK WITH OTHER METHODS ON THE MOT17 TEST SET.

Tracker	HOTA \uparrow	MOTA \uparrow	IDF1 \uparrow	FP \downarrow	FN \downarrow	IDs \downarrow	FPS \uparrow
<i>enhance motion :</i>							
TubeTK [52]	48.0	63.0	58.6	27060	177483	4137	3.0
CenterTrack [45]	52.2	67.8	64.7	18498	160332	3039	17.5
TraDes [46]	52.7	69.1	63.9	20892	150060	3555	17.5
MAT [53]	53.8	69.5	63.1	30660	138741	2844	9.0
PermaTrackPr [54]	55.5	73.8	68.9	28998	115104	3699	11.9
OC-SORT [55]	63.2	78.0	77.5	15129	107055	1950	29.0
MotionTrack [37]	65.1	81.1	80.1	23802	81660	1140	15.7
<i>embedding :</i>							
DAN [56]	39.3	52.4	49.5	25423	234592	8431	<3.9
QuasiDense [17]	53.9	68.7	66.3	26589	146643	3378	20.3
SOTMOT [57]	-	71.0	71.9	39537	118983	5184	16.0
Semi-TCL [19]	59.8	73.3	73.2	22944	124980	2790	-
FairMOT [32]	59.3	73.7	72.3	27507	117477	3303	25.9
CSTrack [33]	59.3	74.9	72.6	23847	114303	3567	15.8
SiamMOT [58]	-	76.3	72.3	-	-	-	12.8
ReMOT [59]	59.7	77.0	72.0	33204	93612	2853	1.8
StrongSORT [44]	64.4	79.6	79.5	27876	86205	1194	7.1
BoT-SORT-ReID [34]	65.0	80.5	80.2	22521	86037	1212	4.5
<i>attention :</i>							
CTracker [60]	49.0	66.6	57.4	22284	160491	5529	6.8
TransCenter [7]	54.5	73.2	62.2	23112	123738	4614	1.0
RelationTrack [61]	61.0	73.8	74.7	27999	118623	1374	8.5
TransTrack [8]	54.1	75.2	63.5	50157	86442	3603	10.0
MOTRv2 [12]	62.0	78.6	75.0	23409	94797	2619	7.5
P3AFormer [10]	-	81.2	78.1	17281	86861	1893	-
<i>graphical & correlation :</i>							
GSDT [62]	55.2	73.2	66.5	26397	120666	3891	4.9
FUFET [63]	57.9	76.2	68.0	32796	98475	3237	6.8
CorrTracker [64]	60.7	76.5	73.6	29808	99510	3369	15.6
TransMOT [9]	61.7	76.7	75.1	36231	93150	2346	9.6
<i>IoU only :</i>							
ByteTrack [6]	63.1	80.3	77.3	25491	83721	2196	29.6
BoT-SORT [34]	64.6	80.6	79.5	22524	85398	1257	6.6
SparseTrack (ours)	65.1	81.0	80.1	23904	81927	1170	19.9

tion results are based on the private detection protocol and are shown in Tab. I, Tab. II and Tab. III, respectively ¹.

MOT17. By performing the target set decomposition based on pseudo-depth, SparseTrack achieves impressive performance on the MOT17 test set. Compared to the baseline (ByteTrack) with the same training settings, SparseTrack achieves gains of **+0.7** MOTA, **+2.8** IDF1, **+2.0** HOTA and IDs decrease to almost twice the original level. Instead of other methods that use appearance features and graph convolutional networks, SparseTrack achieves comparable performance with SOTA using only simple IoU association, which demonstrates that SparseTrack is simply and strong.

MOT20. Compared to MOT17, MOT20 has denser scenes, more occlusions, and longer videos, which increases the difficulty of the tracker in handling occlusions. SparseTrack uses the same training settings as the baseline and achieves a gain of **+0.4** MOTA, **+2.1** IDF1, and **+2.1** HOTA. Compared to other methods that utilize appearance cues, attention mechanism [66], [67] and graph [68]–[70], SparseTrack provides a more convenient solution: the target set decomposition based on

¹The best results are shown with bold in Tab. I, Tab. II and Tab. III. In Tab. III, * indicates that the tracker utilize extra training data.

TABLE II
THE COMPARISON OF SPARSETRACK WITH OTHER METHODS ON THE MOT20 TEST SET.

Tracker	HOTA \uparrow	MOTA \uparrow	IDF1 \uparrow	FP \downarrow	FN \downarrow	IDs \downarrow	FPS \uparrow
<i>enhance motion :</i>							
MotionTrack [37]	62.8	78.0	76.5	28629	84152	1165	15.0
<i>embedding :</i>							
FairMOT [32]	54.6	61.8	67.3	103440	88901	5243	13.2
Semi-TCL [19]	55.3	65.2	70.1	61209	114709	4139	-
CSTrack [33]	54.0	66.6	68.6	25404	144358	3196	4.5
SiamMOT [58]	-	67.1	69.1	-	-	-	4.3
SOTMOT [57]	-	68.6	71.4	57064	101154	4209	8.5
BoT-SORT-ReID [34]	63.3	77.8	77.5	24638	88863	1257	2.4
UTM [18]	62.5	78.2	76.9	29964	81516	1228	-
<i>attention :</i>							
TransCenter [7]	-	61.9	50.4	45895	146347	4653	1.0
TransTrack [8]	48.5	65.0	59.4	27197	150197	3608	7.2
RelationTrack [61]	56.5	67.2	70.5	61134	104597	4243	2.7
MOTR [11]	57.8	73.4	68.6	-	-	2439	-
P3AFormer [10]	-	78.1	76.4	25413	86510	1332	-
<i>graphical & correlation :</i>							
MLT [65]	43.2	48.9	54.6	45660	216803	2187	3.7
CorrTracker [64]	-	65.2	69.1	79429	95855	5183	8.5
GSDT [62]	53.6	67.1	67.5	31913	135409	3131	0.9
<i>IoU only :</i>							
ByteTrack [6]	61.3	77.8	75.2	26249	87594	1223	17.5
BoT-SORT [34]	62.6	77.7	76.3	22521	86037	1212	6.6
SparseTrack (ours)	63.4	78.2	77.3	25108	86720	1116	12.5

TABLE III
THE COMPARISON OF SPARSETRACK WITH OTHER METHODS ON THE DANCETRACK TEST SET.

Tracker	HOTA \uparrow	MOTA \uparrow	IDF1 \uparrow	AssA \uparrow	DetA \uparrow
<i>enhance motion :</i>					
CenterTrack [45]	41.8	86.8	35.7	22.6	78.1
TraDes [46]	43.3	86.2	41.2	25.4	74.5
OC-SORT [55]	55.1	92.0	54.6	38.3	80.3
<i>embedding :</i>					
FairMOT [32]	39.7	82.2	40.8	23.8	66.7
FCG* [71]	48.7	89.9	46.5	29.9	79.8
QuasiDense [17]	54.2	87.7	50.4	36.8	80.1
<i>attention :</i>					
TransTrack [8]	45.5	88.4	45.2	27.5	75.9
GTR [72]	48.0	84.7	50.3	31.9	72.5
MOTR [11]	54.2	79.7	51.5	40.2	73.5
<i>IoU only :</i>					
ByteTrack [6]	47.7	89.6	53.9	32.1	71.0
SparseTrack (ours)	55.5	91.3	58.3	39.1	78.9

hierarchical depth. It is worth mentioning that SparseTrack achieves very low IDs and FP, as well as high HOTA, which indicates that the target set decomposition is helpful in associating dense occlusions.

DanceTrack. DanceTrack is a more challenging benchmark for multi-object tracking with frequent occlusions, non-rigid motions and similar appearances. Under the same weights and training settings, SparseTrack achieves significant improvements compared to the baseline with a gain of **+7.8** HOTA, **+1.7** MOTA, **+4.4** IDF1, **+7.0** AssA and **+7.9** DetA, which demonstrates the enormous potential of depth-based target set decomposition in handling occlusions. Even with simple IoU

distance association, SparseTrack still achieves comparable or even better performance than other methods.

C. Ablations

1) *The efficiency of DCM:* We integrate the DCM module into the baseline [6] to validate the effectiveness of handling low-score occlusions. Specifically, we incorporate DCM into the process of associating low-score detections in ByteTrack. The comparative results of experiments are shown in Tab. IV, where we set the number of pseudo-depth levels to 7 in DCM.

In the MOT17 validation set, by incorporating DCM, the tracker gets an improvement of **+0.7** in HOTA, **+1.4** in AssA, and **+1.6** in IDF1, while the number of IDs is effectively reduced. The results signify the ability of DCM to enhance the tracker capability in associating low-scoring detections within congested scenarios. We further examine the performance of DCM in the MOT20 validation set, which contains more challenging occlusion scenarios. By introducing DCM, the tracker achieves a gain of **+0.5** in HOTA, **+1.1** in AssA, and **+1.0** in IDF1, with minimum changes observed in MOTA and DetA². These results indicate that DCM based the target set decomposition enables the tracker to effectively handle crowded low-score occlusions in demanding scenarios with a lot of occlusion challenges.

2) *The impact of the number of pseudo-depth levels:* We investigate the impact of the number of pseudo-depth levels on the SparseTrack association performance on both the MOT17 validation set and the MOT20 validation set. The experimental results are shown in Tab. V. Specifically, we set the number of pseudo-depth levels for the process of associating low-score detections to 2, 4, 6, 8, separately.

On the MOT17 validation set, the association performance of SparseTrack gradually improves with the increase of the number of pseudo-depth levels. This indicates that a higher number of pseudo-depth levels is more beneficial to associate low-score occlusions. We observe that the performance of the tracker does not show a significant improvement when the number of levels exceeds 6. This suggests that when the number of levels is 6, the partition of the low-score occlusion target set is already sparse enough. We also perform the same experiment with the same settings on the MOT20 validation set and obtain consistent results.

3) *Evaluation of different trackers DCM integrated:* To further explore the effect of target set decomposition on tracking performance, we integrate DCM into seven different trackers to evaluate tracking performance on the MOT17 validation set, including JDE [31], FairMOT [32], CSTrack [33], CenterTrack [45], MOTR [11], TransTrack [8], and TraDes [46]. JDE, FairMOT and CSTrack use appearance embedding as tracking cues. CenterTrack and TraDes use enhanced motion prediction to improve association robustness. TransTrack and MOTR leverage attention mechanism to enhance tracking performance. All experimental results are shown in Tab. VI.

²MOTA reflects detection performance and we use identical detection settings to ensure a fair comparison. The differences in MOTA and DetA metrics in Tab. IV are negligible.

TABLE IV
COMPARISON OF INTEGRATING DCM ALGORITHM ON MOT17 AND MOT20 VALIDATION SETS.

Baseline	w/ DCM	MOT17					MOT20				
		HOTA \uparrow	AssA \uparrow	DetA \uparrow	MOTA \uparrow	IDF1 \uparrow	IDs \downarrow	HOTA \uparrow	AssA \uparrow	DetA \uparrow	MOTA \uparrow
BYTE		68.1	70.0	66.7	76.4	79.4	504	69.3	66.5	72.2	86.1
BYTE	✓	68.8	71.4	66.8	76.7	81.0	384	69.8	67.6	72.2	86.0

TABLE V
COMPARISON OF THE ASSOCIATION PERFORMANCE WITH DIFFERENT NUMBERS OF THE PSEUDO-DEPTH LEVEL
ON MOT17 AND MOT20 VALIDATION SETS.

Method	Levels	MOT17				MOT20			
		HOTA \uparrow	AssA \uparrow	IDF1 \uparrow	IDs \downarrow	HOTA \uparrow	AssA \uparrow	IDF1 \uparrow	IDs \downarrow
Sparse	2	68.3	70.4	80.2	444	69.6	67.2	83.5	991
Sparse	4	68.5	70.7	80.3	444	69.7	67.5	83.7	991
Sparse	6	68.6	70.9	80.3	435	69.8	67.5	83.8	984
Sparse	8	68.6	70.9	80.4	435	69.8	67.5	83.7	988

The specific implementation details will be described in the following³.

Integrating DCM into CenterTrack. CenterTrack is a simple and efficient tracker that utilizes learnable motion prediction based on center point of object to compensate for object motion between adjacent frames and performs data association in frame-by-frame. It's worth noting that CenterTrack only performs single-stage point-based euclidean distance data association. We integrate DCM into the center point distance association process and use IoU distance metric instead of point-based euclidean distance metric. By incorporating DCM, CenterTrack achieved a gain of **+0.3** MOTA and **+2.6** IDF1, as well as a reduction in the number of IDs.

Integrating DCM into JDE. JDE is the first MOT framework for detection and tracking simultaneously, following the tracking-by-detection paradigm. Firstly, JDE outputs detections and embeddings simultaneously through a detector and then performs data association in a tracking post-processing step. Since JDE uses an anchor-based detector [74], [76]–[81], detections and embeddings are not associated in a one-to-one relationship. Therefore, we only integrate DCM into the IoU association step of JDE, while keeping the embedding association unchanged, resulting in a gain of **+1.4** IDF1. Based on this, we also attempt to replace the embedding association process in JDE with IoU-based DCM, resulting in a gain of **+0.1** MOTA and **+1.9** IDF1 compared with original JDE.

Integrating DCM into FairMOT. Comparing with JDE, FairMOT adopts an independent embedding branch to predict appearance features. FairMOT also uses an anchor-free detector [43], [82], [83] to ensure that a detection corresponds to only one appearance embedding, which ensures the fairness

between detection and appearance prediction to a certain extent. We integrate DCM into the IoU-based association process of FairMOT and achieve a gain of **+0.3** MOTA and **+0.5** IDF1. In addition, we also replace the embedding association process of FairMOT with IoU-bassed DCM, which results in a gain of **+1.2** MOTA, **+1.1** IDF1 for the tracker.

Integrating DCM into CStrack. CStrack rethinks the fairness between the detection and ReID tasks. It believes that sharing network parameters and structures for both tasks would lead to a competitive relationship. To address this issue, CStrack decouples the detection and ReID tasks based on the JDE framework by a correlation learning structure. Additionally, CStrack introduces multi-scale feature enhancement specifically designed for the ReID task. We replace the position association process in CStrack with DCM, resulting in a gain of **+0.6** MOTA and **+1.6** IDF1. Similar to the above approach, we substitute the embedding association process in CStrack with DCM based on the IoU distance metric, achieving an improvement of **+0.5** MOTA and **+0.6** IDF1.

Integrating DCM into TraDes. TraDes enhances the motion cues and ReID embeddings in the tracking process through the Cost Volume based Association (CVA) module and Motion-guided Feature Warper (MFW) module. The CVA module is used for learning ReID embeddings and generating motion predictions of targets, which is similar to CenterTrack. The MFW module propagates and enhances the features of the targets based on the motion and tracking cues generated by CVA. It should be mentioned that TraDes introduces the IoU distance metric into the location association process compared with CenterTrack. Based on this, we incorporate DCM into the location matching process of TraDes, which can get a gain of **+0.1** MOTA, **+1.0** IDF1.

Integrating DCM into TransTrack. TransTrack is the first approach that incorporates query-based framework [84] into multi-object tracking task while still following the tracking-by-detection paradigm. Firstly, it extracts image features using a CNN backbone [41], [85] and aggregates the features of the current frame and the previous frame before passing them to an encoder-decoder module. TransTrack utilizes the deformable

³All experiments in Tab. VI are performed on the MOT17 validation set, which includes all video sequences with suffixes DPM [73], FRCNN [74], and SDP [75]. **IoU(K)** represents the use of the Kalman filter motion model and IoU distance metric during the association stage. **ReID** indicates the utilization of appearance embedding similarity during the association stage. **Motion** denotes the application of enhanced motion prediction during the association stage. **Attention** signifies that data association benefits from the attention mechanism derived from the transformer framework. All the gains brought by DCM are highlighted in red font.

TABLE VI
COMPARISON OF INTEGRATING DCM ALGORITHM INTO DIFFERENT TRACKERS.

Trackers	Method	w/ DCM	MOTA↑	IDF1↑	IDs↓
JDE [31]	IoU(K) + Re-ID		60.0	63.6	1425
	IoU(K) + Re-ID	✓	60.0	65.0 (+1.4)	1356
	IoU(K)	✓	60.1 (+0.1)	65.5 (+1.9)	1215
CSTrack [33]	IoU(K) + Re-ID		68.0	72.2	1215
	IoU(K) + Re-ID	✓	68.6 (+0.6)	73.8 (+1.6)	1032
	IoU(K)	✓	68.5 (+0.5)	72.8 (+0.6)	924
FairMOT [32]	IoU(K) + Re-ID		69.1	72.8	900
	IoU(K) + Re-ID	✓	69.4 (+0.3)	73.3 (+0.5)	1119
	IoU(K)	✓	70.3 (+1.2)	73.9 (+1.1)	690
TraDes [46]	Motion + Re-ID		68.2	71.6	858
	Motion + Re-ID	✓	68.3 (+0.1)	72.6 (+1.0)	909
CenterTrack [45]	Motion		66.1	64.3	1608
	Motion	✓	66.4 (+0.3)	66.9 (+2.6)	807
TransTrack [8]	Attention		67.1	70.1	771
	Attention	✓	67.0 (-0.1)	71.4 (+1.3)	1032
MOTR [11]	Attention		65.0	67.1	1068
	Attention	✓	64.7 (-0.3)	69.6 (+2.5)	801

attention [86] during the encoding and decoding process. Particularly, TransTrack employs two kinds of decoders to obtain detection information for the current frame and predictions from previous frame trajectories, separately. Since TransTrack requires both current and previous frame features during a tracking stage, it adopts a multi-frame training approach during the training phase. During the data association stage, TransTrack utilizes the GIoU [87] distance metric for position association, similar to CenterTrack. We integrate DCM into the position association process and replace the original GIoU metric with a simple IoU metric, resulting in a gain of **+1.3** IDF1.

Integrating DCM into MOTR. MOTR is an end-to-end multi-object tracker based on the transformer architecture. By utilizing a temporal aggregation network (TAN) to model long-term temporal variations of objects, MOTR performs implicit temporal association and avoids explicitly heuristic strategies used by aforementioned previous trackers. Benefiting from the DETR framework, MOTR introduces the track query and detection query during the tracking process. Track queries are responsible for maintaining existing trajectories, while detection queries are used to discover newly appearing objects in each frame. Through the combination of trajectory queries and detection queries, MOTR achieves robust tracking performance with end-to-end paradigm. Due to the implicit association paradigm, MOTR is trained in a multi-frames mode to capture long-term temporal relationships. We introduce the tracking post process based on DCM into MOTR, which results in the association improvement of **+2.5** IDF1.

D. Visualization

To exhibiting the target set decomposition process and the performance of associating crowded targets intuitively, we

conduct several different visualization experiments, as shown in Fig. 6, Fig. 7 and Fig. 8, respectively.

Visualization of the target set decomposition. Although the target set decomposition is a sub-process of DCM, it is the key to decoupling dense occlusions. In fact, not all targets in the scene are occluded state, but occluded targets may gather together and form dense occlusions easier, as shown in Fig. 6. By decomposing dense occlusion set based on pseudo-depth information, overlapping targets can be assigned to different depth levels, effectively. We visualize the decomposition of a set of dense occlusions, as shown in Fig. 7.

Visualization of associating crowded targets. SparseTrack associates low-score dense occlusions based on the correlation between depth order and occlusion order instead of associating all low-score dense occlusions simply. It can enable occluded targets located at different depth levels to be associated as much as possible. Visualized results Fig. 8 prove that our method helps stabilize the trajectories of occluded targets.

E. Limits

Despite achieving excellent performance in MOT scenarios, SparseTrack faces challenges in other demanding scenarios such as [15], [88] where targets exhibit rapid motion and deformation. In such cases, it becomes difficult for the pseudo-depth method to capture the relative depth relationships accurately, which affects the tracking performance of SparseTrack. Additionally, for videos with low frame rates [89], simple Kalman filter motion model struggles to obtain accurate motion cues. In the future work, we will explore the different decomposition methods that can be adapted to various tracking scenarios and aim to make the implementation more elegant.

V. CONCLUSION

We propose a simple tracker for multi-object tracking named as SparseTrack. It leverages the pseudo-depth method to estimate the relative depth relationship between different targets and divides the target set into multiple sparse subsets in order of increasing depth. To associate occluded targets distributed across these sparse subsets, we introduce the Depth Cascade Matching (DCM) algorithm, which performs the association between detection subsets and trajectory subsets at the same depth level. Compared to previous tracking methods, SparseTrack offers a different perspective on addressing occlusion: the target set decomposition, which partitions the dense target set into sparse subsets by pseudo-depth information. SparseTrack achieves competitive performance on the MOT17 and MOT20 datasets comparing to state-of-the-art methods via solely utilizing simple IoU distance association, without relying on robust appearance embeddings or enhanced motion prediction. This demonstrates the effectiveness of decomposition based on depth information. It is worth noting that DCM is plug-and-play and can be integrated into any existing tracker, yielding consistent performance improvements. We hope that SparseTrack can provide alternative solutions for multi-object tracking tasks and inspire the development of more powerful and elegant approaches based on the concept of **sparsity** in the future.

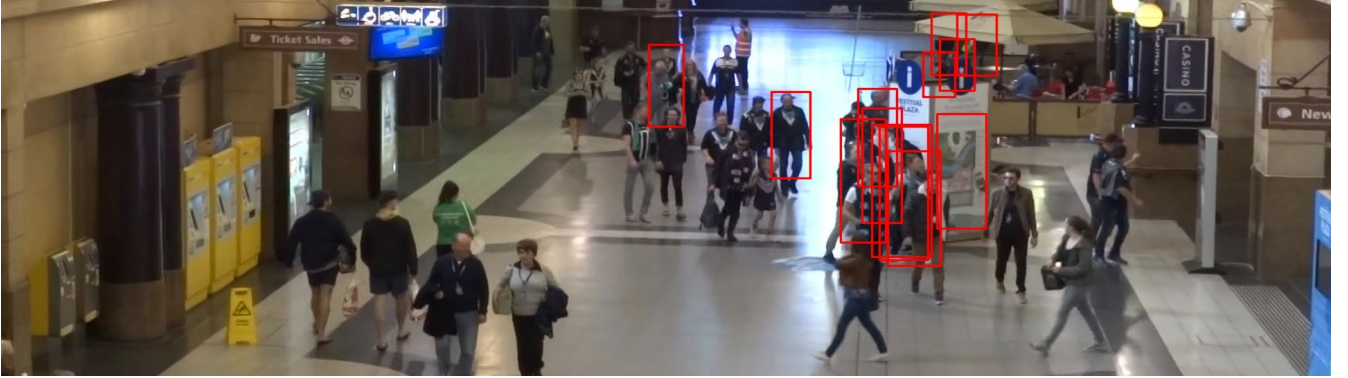


Fig. 6. Visualization of dense occlusions. We visualize ground truth instances with visibility less than 0.15. The occluded targets in the crowd are often clustered, resulting in dense occlusions.



Fig. 7. Visualization of decomposing dense occlusions. We use different color of bounding boxes to distinguish different target subsets obtained via dividing pseudo-depth levels.



Fig. 8. Visualization of associating crowded targets. We visualize the partial tracking results of SparseTrack on the MOT20 test set. To clarify the targets of trajectory, we use a red point at the first frame of each video clip to mark the uncovered parts of the target.

ACKNOWLEDGMENTS

We thank Yifu Zhang, Bencheng Liao, Jiemin Fang, Yunchi Zhang, and Jinfeng Yao for their insightful discussions and suggestions. This work is in part supported by the National Key Research and Development Program of China under Grant

2022YFB4500602.

REFERENCES

[1] S. Vandenhende, S. Georgoulis, W. Van Gansbeke, M. Proesmans, D. Dai, and L. Van Gool, “Multi-task learning for dense prediction

tasks: A survey,” *IEEE Transactions on Pattern Analysis and Machine Intelligence*, 2021. 1

[2] L. Leal-Taixé, A. Milan, I. Reid, S. Roth, and K. Schindler, “MOTChallenge 2015: Towards a benchmark for multi-target tracking,” *arXiv:1504.01942 [cs]*, Apr. 2015, arXiv: 1504.01942. [Online]. Available: <http://arxiv.org/abs/1504.01942> 1, 2

[3] A. Milan, L. Leal-Taixé, I. Reid, S. Roth, and K. Schindler, “Mot16: A benchmark for multi-object tracking,” *arXiv preprint arXiv:1603.00831*, 2016. 1, 2, 6

[4] P. Dendorfer, H. Rezatofighi, A. Milan, J. Shi, D. Cremers, I. Reid, S. Roth, K. Schindler, and L. Leal-Taixé, “Mot20: A benchmark for multi object tracking in crowded scenes,” *arXiv preprint arXiv:2003.09003*, 2020. 1, 2, 6

[5] A. Bewley, Z. Ge, L. Ott, F. Ramos, and B. Upcroft, “Simple online and realtime tracking,” in *2016 IEEE International Conference on Image Processing (ICIP)*, 2016, pp. 3464–3468. 1, 2

[6] Y. Zhang, P. Sun, Y. Jiang, D. Yu, F. Weng, Z. Yuan, P. Luo, W. Liu, and X. Wang, “Bytetrack: Multi-object tracking by associating every detection box,” 2022. 1, 3, 5, 6, 7

[7] Y. Xu, Y. Ban, G. Delorme, C. Gan, D. Rus, and X. Alameda-Pineda, “Transcenter: Transformers with dense queries for multiple-object tracking,” *arXiv preprint arXiv:2103.15145*, 2021. 1, 6, 7

[8] P. Sun, Y. Jiang, R. Zhang, E. Xie, J. Cao, X. Hu, T. Kong, Z. Yuan, C. Wang, and P. Luo, “Trantrack: Multiple-object tracking with transformer,” *arXiv preprint arXiv:2012.15460*, 2020. 1, 6, 7, 9

[9] P. Chu, J. Wang, Q. You, H. Ling, and Z. Liu, “Transmot: Spatial-temporal graph transformer for multiple object tracking,” *arXiv preprint arXiv:2104.00194*, 2021. 1, 6

[10] Z. Zhao, Z. Wu, Y. Zhuang, B. Li, and J. Jia, “Tracking objects as pixel-wise distributions,” 2022. 1, 6, 7

[11] F. Zeng, B. Dong, Y. Zhang, T. Wang, X. Zhang, and Y. Wei, “Motr: End-to-end multiple-object tracking with transformer,” in *European Conference on Computer Vision (ECCV)*, 2022. 1, 2, 3, 7, 9

[12] Y. Zhang, T. Wang, and X. Zhang, “Motrv2: Bootstrapping end-to-end multi-object tracking by pretrained object detectors,” *Computer Vision and Pattern Recognition CVPR*, 2023. 1, 2, 6

[13] R. Girshick, J. Donahue, T. Darrell, and J. Malik, “Rich feature hierarchies for accurate object detection and semantic segmentation,” in *Computer Vision and Pattern Recognition (CVPR)*, 2014. 2

[14] J. Luiten, A. Osep, P. Dendorfer, P. Torr, A. Geiger, L. Leal-Taixé, and B. Leibe, “Hota: A higher order metric for evaluating multi-object tracking,” *International journal of computer vision*, vol. 129, no. 2, pp. 548–578, 2021. 2, 6

[15] P. Sun, J. Cao, Y. Jiang, Z. Yuan, S. Bai, K. Kitani, and P. Luo, “Dancetrack: Multi-object tracking in uniform appearance and diverse motion,” *arXiv preprint arXiv:2111.14690*, 2021. 2, 6, 9

[16] Z. Wang, H. Zhao, Y.-L. Li, S. Wang, P. Torr, and L. Bertinetto, “Do different tracking tasks require different appearance models?” *Thirty-Fifth Conference on Neural Information Processing Systems*, 2021. 2

[17] J. Pang, L. Qiu, X. Li, H. Chen, Q. Li, T. Darrell, and F. Yu, “Quasi-dense similarity learning for multiple object tracking,” in *IEEE/CVF Conference on Computer Vision and Pattern Recognition*, June 2021. 2, 4, 6, 7

[18] S. You, H. Yao, B.-K. Bao, and C. Xu, “Utm: A unified multiple object tracking model with identity-aware feature enhancement,” *Computer Vision and Pattern Recognition (CVPR)*, 2023. 2, 7

[19] W. Li, Y. Xiong, S. Yang, M. Xu, Y. Wang, and W. Xia, “Semi-tcl: Semi-supervised track contrastive representation learning,” *arXiv preprint arXiv:2107.02396*, 2021. 2, 6, 7

[20] L. He, X. Liao, W. Liu, X. Liu, P. Cheng, and T. Mei, “Fastreid: A pytorch toolbox for general instance re-identification,” *arXiv preprint arXiv:2006.02631*, 2020. 2

[21] K. Zhou and T. Xiang, “Torchreid: A library for deep learning person re-identification in pytorch,” *arXiv preprint arXiv:1910.10093*, 2019. 2

[22] K. Zhou, Y. Yang, A. Cavallaro, and T. Xiang, “Omni-scale feature learning for person re-identification,” in *ICCV*, 2019. 2

[23] ——, “Learning generalisable omni-scale representations for person re-identification,” 2021. 2

[24] K. He, H. Fan, Y. Wu, S. Xie, and R. Girshick, “Momentum contrast for unsupervised visual representation learning,” *arXiv preprint arXiv:1911.05722*, 2019. 2

[25] X. Chen, H. Fan, R. Girshick, and K. He, “Improved baselines with momentum contrastive learning,” *arXiv preprint arXiv:2003.04297*, 2020. 2

[26] T. Chen, S. Kornblith, M. Norouzi, and G. Hinton, “A simple framework for contrastive learning of visual representations,” *arXiv preprint arXiv:2002.05709*, 2020. 2

[27] T. Chen, S. Kornblith, K. Swersky, M. Norouzi, and G. Hinton, “Big self-supervised models are strong semi-supervised learners,” *arXiv preprint arXiv:2006.10029*, 2020. 2

[28] K. He, X. Chen, S. Xie, Y. Li, P. Dollár, and R. Girshick, “Masked autoencoders are scalable vision learners,” *arXiv:2111.06377*, 2021. 2

[29] N. Wojke, A. Bewley, and D. Paulus, “Simple online and realtime tracking with a deep association metric,” in *2017 IEEE International Conference on Image Processing (ICIP)*. IEEE, 2017, pp. 3645–3649. 2, 3, 4

[30] C. Long, A. Haizhou, Z. Zijie, and S. Chong, “Real-time multiple people tracking with deeply learned candidate selection and person re-identification,” in *ICME*, 2018. 2

[31] Z. Wang, L. Zheng, Y. Liu, and S. Wang, “Towards real-time multi-object tracking,” *The European Conference on Computer Vision (ECCV)*, 2020. 2, 7, 9

[32] Y. Zhang, C. Wang, X. Wang, W. Zeng, and W. Liu, “Fairmot: On the fairness of detection and re-identification in multiple object tracking,” *International Journal of Computer Vision*, vol. 129, pp. 3069–3087, 2021. 2, 3, 4, 6, 7, 9

[33] C. Liang, Z. Zhang, X. Zhou, B. Li, S. Zhu, and W. Hu, “Rethinking the competition between detection and reid in multiobject tracking,” *IEEE Trans Image Process*, pp. 3182–3196, 2022. 2, 4, 6, 7, 9

[34] N. Aharon, R. Orfaig, and B.-Z. Bobrovsky, “Bot-sort: Robust associations multi-pedestrian tracking,” *arXiv preprint arXiv:2206.14651*, 2022. 2, 3, 6, 7

[35] C. Feichtenhofer, A. Pinz, and A. Zisserman, “Detect to track and track to detect,” in *International Conference on Computer Vision (ICCV)*, 2017. 2

[36] K. RE, “A new approach to linear filtering and prediction problems.” *J Fluids Eng*, vol. 82, no. 1, pp. 35–45, 1960. 2

[37] Z. Qin, S. Zhou, L. Wang, J. Duan, G. Hua, and W. Tang, “Motiontrack: Learning robust short-term and long-term motions for multi-object tracking,” *Computer Vision and Pattern Recognition (CVPR)*, 2023. 3, 6, 7

[38] B. Mildenhall, P. P. Srinivasan, M. Tancik, J. T. Barron, R. Ramamoorthi, and R. Ng, “Nerf: Representing scenes as neural radiance fields for view synthesis,” in *ECCV*, 2020. 3

[39] P. Voigtlaender, M. Krause, A. Osep, J. Luiten, B. B. G. Sekar, A. Geiger, and B. Leibe, “MOTS: Multi-object tracking and segmentation,” in *CVPR*, 2019. 3

[40] E. Baser, V. Balasubramanian, P. Bhattacharyya, and K. Czarnecki, “Fantrack: 3d multi-object tracking with feature association network,” in *IEEE Intelligent Vehicles Symposium (IV 19)*, 2019. 3

[41] A. Krizhevsky, I. Sutskever, and G. E. Hinton, “Imagenet classification with deep convolutional neural networks,” *NIPS*, 2012. 3, 8

[42] T. Yin, X. Zhou, and P. Krähenbühl, “Center-based 3d object detection and tracking,” *CVPR*, 2021. 3

[43] Z. Ge, S. Liu, F. Wang, Z. Li, and J. Sun, “Yolox: Exceeding yolo series in 2021,” *arXiv preprint arXiv:2107.08430*, 2021. 3, 6, 8

[44] Y. Du, Y. Song, B. Yang, and Y. Zhao, “Strongsort: Make deepsort great again,” *arXiv preprint arXiv:2202.13514*, 2022. 4, 6

[45] X. Zhou, V. Koltun, and P. Krähenbühl, “Tracking objects as points,” *ECCV*, 2020. 4, 6, 7, 9

[46] J. Wu, J. Cao, L. Song, Y. Wang, M. Yang, and J. Yuan, “Track to detect and segment: An online multi-object tracker,” in *Proceedings of the IEEE/CVF Conference on Computer Vision and Pattern Recognition*, 2021, pp. 12 352–12 361. 4, 6, 7, 9

[47] K. Bernardin and R. Stiefelhagen, “Evaluating multiple object tracking performance: the clear mot metrics,” *EURASIP Journal on Image and Video Processing*, vol. 2008, pp. 1–10, 2008. 6

[48] E. Ristani, F. Solera, R. Zou, R. Cucchiara, and C. Tomasi, “Performance measures and a data set for multi-target, multi-camera tracking,” in *ECCV*. Springer, 2016, pp. 17–35. 6

[49] A. Ess, B. Leibe, K. Schindler, and L. Van Gool, “A mobile vision system for robust multi-person tracking,” in *CVPR*. IEEE, 2008, pp. 1–8. 6

[50] S. Shao, Z. Zhao, B. Li, T. Xiao, G. Yu, X. Zhang, and J. Sun, “Crowdhuman: A benchmark for detecting human in a crowd,” *arXiv preprint arXiv:1805.00123*, 2018. 6

[51] S. Zhang, R. Benenson, and B. Schiele, “Citypersons: A diverse dataset for pedestrian detection,” in *CVPR*, 2017, pp. 3213–3221. 6

[52] B. Pang, Y. Li, Y. Zhang, M. Li, and C. Lu, “Tubetk: Adopting tubes to track multi-object in a one-step training model,” in *Proceedings of the IEEE/CVF Conference on Computer Vision and Pattern Recognition*, 2020, pp. 6308–6318. 6

[53] S. Han, P. Huang, H. Wang, E. Yu, D. Liu, X. Pan, and J. Zhao, “Mat: Motion-aware multi-object tracking,” *arXiv preprint arXiv:2009.04794*, 2020. 6

[54] P. Tokmakov, J. Li, W. Burgard, and A. Gaidon, “Learning to track with object permanence,” *arXiv preprint arXiv:2103.14258*, 2021. 6

[55] J. Cao, X. Weng, R. Khirodkar, J. Pang, and K. Kitani, “Observation-centric sort: Rethinking sort for robust multi-object tracking,” *arXiv preprint arXiv:2203.14360*, 2022. 6, 7

[56] S. Sun, N. Akhtar, H. Song, A. S. Mian, and M. Shah, “Deep affinity network for multiple object tracking,” *IEEE transactions on pattern analysis and machine intelligence*, 2019. 6

[57] L. Zheng, M. Tang, Y. Chen, G. Zhu, J. Wang, and H. Lu, “Improving multiple object tracking with single object tracking,” in *Proceedings of the IEEE/CVF Conference on Computer Vision and Pattern Recognition*, 2021, pp. 2453–2462. 6, 7

[58] B. Shuai, A. Berneshawi, X. Li, D. Modolo, and J. Tighe, “Siammot: Siamese multi-object tracking,” in *Proceedings of the IEEE/CVF Conference on Computer Vision and Pattern Recognition*, 2021, pp. 12372–12382. 6, 7

[59] F. Yang, X. Chang, S. Sakti, Y. Wu, and S. Nakamura, “Remot: A model-agnostic refinement for multiple object tracking,” *Image and Vision Computing*, vol. 106, p. 104091, 2021. 6

[60] J. Peng, C. Wang, F. Wan, Y. Wu, Y. Wang, Y. Tai, C. Wang, J. Li, F. Huang, and Y. Fu, “Chained-tracker: Chaining paired attentive regression results for end-to-end joint multiple-object detection and tracking,” in *Proceedings of the European Conference on Computer Vision*, 2020. 6

[61] E. Yu, Z. Li, S. Han, and H. Wang, “Relationtrack: Relation-aware multiple object tracking with decoupled representation,” *arXiv preprint arXiv:2105.04322*, 2021. 6, 7

[62] Y. Wang, K. Kitani, and X. Weng, “Joint object detection and multi-object tracking with graph neural networks,” *arXiv preprint arXiv:2006.13164*, 2020. 6, 7

[63] C. Shan, C. Wei, B. Deng, J. Huang, X.-S. Hua, X. Cheng, and K. Liang, “Tracklets predicting based adaptive graph tracking,” *arXiv preprint arXiv:2010.09015*, 2020. 6

[64] Q. Wang, Y. Zheng, P. Pan, and Y. Xu, “Multiple object tracking with correlation learning,” in *Proceedings of the IEEE/CVF Conference on Computer Vision and Pattern Recognition*, 2021, pp. 3876–3886. 6, 7

[65] Y. Zhang, H. Sheng, Y. Wu, S. Wang, W. Ke, and Z. Xiong, “Multiplex labeling graph for near-online tracking in crowded scenes,” *IEEE Internet of Things Journal*, vol. 7, no. 9, pp. 7892–7902, 2020. 7

[66] A. Vaswani, N. Shazeer, N. Parmar, J. Uszkoreit, L. Jones, A. N. Gomez, Ł. Kaiser, and I. Polosukhin, “Attention is all you need,” in *Advances in neural information processing systems*, 2017, pp. 5998–6008. 6

[67] A. Dosovitskiy, L. Beyer, A. Kolesnikov, D. Weissenborn, X. Zhai, T. Unterthiner, M. Dehghani, M. Minderer, G. Heigold, S. Gelly, J. Uszkoreit, and N. Houlsby, “An image is worth 16x16 words: Transformers for image recognition at scale,” in *International Conference on Learning Representations*, 2021. [Online]. Available: <https://openreview.net/forum?id=YicbFdNTTy> 6

[68] G. Braso and L. Leal-Taixe, “Learning a neural solver for multiple object tracking,” *CVPR*, 2020. 6

[69] J. Li, X. Gao, and T. Jiang, “Graph networks for multiple object tracking,” in *Proceedings of the IEEE/CVF Winter Conference on Applications of Computer Vision (WACV)*, March 2020. 6

[70] J. He, Z. Huang, N. Wang, and Z. Zhang, “Learnable graph matching: Incorporating graph partitioning with deep feature learning for multiple object tracking,” 2021, p. 5299–5309. 6

[71] A. Girbau, F. Marqués, and S. Satoh, “Multiple object tracking from appearance by hierarchically clustering tracklets,” *BMVC*, 2022. 7

[72] X. Zhou, T. Yin, V. Koltun, and P. Krähenbühl, “Global tracking transformers,” in *CVPR*, 2022. 7

[73] P. Felzenszwalb, D. McAllester, and D. Ramanan, “A discriminatively trained, multiscale, deformable part model,” in *CVPR*. IEEE, 2008, pp. 1–8. 8

[74] S. Ren, K. He, R. Girshick, and J. Sun, “Faster R-CNN: Towards real-time object detection with region proposal networks,” *arXiv preprint arXiv:1506.01497*, 2015. 8

[75] F. Yang, W. Choi, and Y. Lin, “Exploit all the layers: Fast and accurate cnn object detector with scale dependent pooling and cascaded rejection classifiers,” in *Proceedings of the IEEE conference on computer vision and pattern recognition*, 2016, pp. 2129–2137. 8

[76] J. Redmon and A. Farhadi, “Yolov3: An incremental improvement,” *arXiv*, 2018. 8

[77] H.-Y. M. L. Alexey Bochkovskiy, Chien-Yao Wang, “Yolov4: Yolov4: Optimal speed and accuracy of object detection,” *arXiv*, 2020. 8

[78] glenn jocher *et al.*, “yolov5,” <https://github.com/ultralytics/yolov5>, 2021. 8

[79] C.-Y. Wang, A. Bochkovskiy, and H.-Y. M. Liao, “YOLOv7: Trainable bag-of-freebies sets new state-of-the-art for real-time object detectors,” *arXiv preprint arXiv:2207.02696*, 2022. 8

[80] R. Girshick, “Fast r-cnn,” in *International Conference on Computer Vision (ICCV)*, 2015. 8

[81] W. Liu, D. Anguelov, D. Erhan, C. Szegedy, S. Reed, C.-Y. Fu, and A. C. Berg, “Ssd: Single shot multibox detector,” in *European conference on computer vision*. Springer, 2016, pp. 21–37. 8

[82] X. Zhou, D. Wang, and P. Krähenbühl, “Objects as points,” in *arXiv preprint arXiv:1904.07850*, 2019. 8

[83] Z. Tian, C. Shen, H. Chen, and T. He, “Fcos: Fully convolutional one-stage object detection,” in *Proceedings of the IEEE/CVF international conference on computer vision*, 2019, pp. 9627–9636. 8

[84] N. Carion, F. Massa, G. Synnaeve, N. Usunier, A. Kirillov, and S. Zagoruyko, “End-to-end object detection with transformers,” in *European conference on computer vision*. Springer, 2020, pp. 213–229. 8

[85] K. He, X. Zhang, S. Ren, and J. Sun, “Deep residual learning for image recognition,” *arXiv preprint arXiv:1512.03385*, 2015. 8

[86] X. Zhu, W. Su, L. Lu, B. Li, X. Wang, and J. Dai, “Deformable {detr}: Deformable transformers for end-to-end object detection,” in *International Conference on Learning Representations*, 2021. [Online]. Available: <https://openreview.net/forum?id=gZ9hCDWe6ke> 9

[87] H. Rezatofighi, N. Tsoi, J. Gwak, A. Sadeghian, I. Reid, and S. Savarese, “Generalized intersection over union: A metric and a loss for bounding box regression,” in *Proceedings of the IEEE/CVF conference on computer vision and pattern recognition*, 2019, pp. 658–666. 9

[88] P. Zhu, L. Wen, D. Du, X. Bian, H. Fan, Q. Hu, and H. Ling, “Detection and tracking meet drones challenge,” *IEEE Transactions on Pattern Analysis and Machine Intelligence*, pp. 1–1, 2021. 9

[89] F. Yu, H. Chen, X. Wang, W. Xian, Y. Chen, F. Liu, V. Madhavan, and T. Darrell, “Bdd100k: A diverse driving dataset for heterogeneous multitask learning,” in *Proceedings of the IEEE/CVF conference on computer vision and pattern recognition*, 2020, pp. 2636–2645. 9